Int. J. Electrochem. Sci., 13 **(2018)** 6930 – 6939, doi: 10.20964/2018.07.18

International Journal of
ELECTROCHEMICAL
SCIENCE
www.electrochemsci.org

Surface Modification of $Li_{1.2}Mn_{0.6}Ni_{0.2}O_2$ with Electronic Conducting Polypyrrole

Hao Wu, Honglei Li, Puheng Yang, Yalan Xing[*]*, Shichao Zhang*[*]

School of Materials Science and Engineering, Beihang University, Beijing 100191, PR China
[*]E-mail: xingyalan@buaa.edu.cn

Received: 24 February 2018 / *Accepted:* 17 April 2018 / *Published:* 5 June 2018

To enhance the initial coulombic efficiency, cyclic stability and electronic conductivity of lithium-rich cathode material $Li_{1.2}Mn_{0.6}Ni_{0.2}O_2$, surface modification is carried out by a facile chemical oxidation polymerization method with pyrrole monomer. The comparison between bare and polypyrrole-coated samples on the structure, morphology and electrochemical properties are investigated and analyzed. Despite sacrificed a part of initial capacity, the initial coulombic efficiency, the cyclic stability and electronic conductivity have been improved.

Keywords: Lithium-rich cathode material; Solvothermal method; Electrochemical performance; surface modification; polypyrrole.

1. INTRODUCTION

Nowadays, lithium-ion batteries (LIBs) are widely engaged in the industry of portable electronic devices (PEDs), electric vehicles, and energy storages. Cathode materials with high energy density and high discharge capacity are expected to satisfy the needs of increasing science and technology. Compared with commercialized cathode materials, such as $LiCoO_2$, $LiFePO_4$ and $Li[Ni_{1/3}Mn_{1/3}Co_{1/3}]O_2$, lithium-rich cathode materials are capable of delivering a higher discharge capacity of above 250 mAh g^{-1}, considered as one of the most promising candidates of cathode materials for lithium ion batteries [1–3]. Furthermore, the layered lithium-rich cathode materials possess high energy and power density, which is necessary in the applications of electric vehicles (EV), hybrid electric vehicles (HEV) and plug-in hybrid electric vehicles (PHEV).

Lithium-rich cathode materials are considered as a solid solution of $LiMO_2$ (M = Mn, Ni, Co) and Li_2MnO_3 in most studies [4,5]. Among these Li-rich materials, $Li_{1.2}Mn_{0.6}Ni_{0.2}O_2$ is particularly worth emphasizing ascribe to environmental benignity, low cost and improved safety, compared with other Li-rich materials containing cobalt element. However, it still suffers from several defects, such as initial irreversible capacity loss, inferior cycle performance and electronic conductivity, which hindered its further application [2].

To alleviate these problems, fabricating nanoparticles and surface modification have been proved as effective strategies [6,7]. The synthetic process had greatly influence in structure, morphology, composition, homogeneity and electrochemical properties of layered Li-rich cathode materials. Therefore, it is effective to find an appropriate method to synthesis nano-sized materials to improve the electrochemical performance. Till now several methods have been used to synthesis layered Li-rich cathode materials, including solid state method [8], co-precipitation method [9], sol-gel method [10], combustion method [1], hydrothermal method [11], spray pyrolysis [12]. Compared with above-mentioned methods, solvothermal method could be more beneficial in the control of crystal growth, morphology, phase purity, and intrinsic defect concentration [13]. It is reported that ethylene glycol as a solvent has high viscosity and could restrict the growth rate of particles [14]. Thus it is easier to synthesize the nano-sized materials with the well-defined morphology, well-ordered structure and good homogeneity [15].

The nanoscale interspaces for nanoparticles can be easily filled with the electrolyte, ensuring a high electrode-electrolyte contact area and a short pathway for Li^+ diffusion. However, active material surface could be corroded by electrolyte at high potentials. Surface modification by polypyrrole (PPy) is an effective method in suppressing electrode-electrolyte contact and the solution of Ni^{4+} thereby improving the cycling stability and coulombic efficiency [16–18]. As conductive polymer, PPy coating could increase the electronic conductivity [19,20].

In this work, Li-rich cathode material $Li_{1.2}Mn_{0.6}Ni_{0.2}O_2$ was synthesized by a solvothermal method with ethylene glycol as solvent, combined with a subsequent calcination process. Surface modification was carried out by a facile chemical oxidation polymerization method. The effects of PPy coating on the microstructure and electrochemical performance of the PPy-LMNO cathode materials are investigated.

2. EXPERIMENTAL

The preparation procedure of pristine $Li_{1.2}Mn_{0.6}Ni_{0.2}O_2$ (LMNO) could be described briefly as follows. 6 mmol manganese chloride ($MnCl_2{\cdot}4H_2O$) and 2 mmol nickel chloride ($NiCl_2{\cdot}6H_2O$) were dissolved in 80 mL ethylene glycol. And 10 mmol ammonium bicarbonate (NH_4HCO_3) was added dropwise to the mixed metal-chloride solution under continuous stirring. After sufficiently mixing, the mixture was transferred into a 100 mL Teflon-lined stainless steel autoclave, which was subsequently

tightened and heated up to 200 °C for 16 h in an electric oven. Then cooled down to room temperature, after gathered and washed with distilled water and ethanol respectively for five times, the precursors were mixed well with stoichiometric amount of Li_2CO_3 (5 wt. % excess). The final product was obtained after presintered and calcined at 900 °C for 12 h in a tubular furnace. All the chemicals were analytically pure and the lithium source should be excess to compensate for lithium loss in high temperature heat treatment.

PPy-coated $Li_{1.2}Mn_{0.6}Ni_{0.2}O_2$ (PPy-LMNO) was prepared by a facile chemical oxidation polymerization method. 0.5g as-prepared pristine material and 0.25g anhydrous iron trichloride were diffused in deionized water under ultrasonic for half of an hour. And then 0.1g liquid pyrrole monomer was added in the aforementioned solution. The solution was then magnetically stirred 24 h to complete the polymerization reaction. The final products were filtered, washed with deionized water several times, and dried at 60 °C for 24 h to obtain the final product PPy-LMNO.

The crystal structure of the as-synthesized material was obrained in the range of 2θ value from 10-80° by powder X-ray diffraction (XRD) on a Rigaku D/Max-2400 diffractometer with Cu Kα radiation. The morphology and microstructure of the sample were observed using a Field-emission scanning electron microscopy (SEM) (Hitachi, model S-4800, Japan) and transmission electron microscopy (TEM) (model JEOL 2010F). A thermal analyzer (NETZSCH, model STA 449F3) was used to perform thermal-gravimetric (TG) analysis of PPy-LMNO. Raman spectrum were obtained by using a LabRam HR 800 (HORIBA).

To measure electrochemical properties of the samples, half cells (model 2032) were assembled in a glove box (MBRAUN, model MB-10-G) with argon atmosphere, and Li metal foil (15.8 mm diameter) was used as the counter and reference electrode. The concentration of H_2O and O_2 were kept less than 1 ppm during the assembly to minimize impact of oxygen and water. The working electrodes were prepared by spreading a mixture of as-prepared Li-rich cathode material (LMNO and PPy-LMNO, 80 wt.%), carbon black (Super P, 10 wt.%), and polyvinylidene fluoride binder(PVDF, 10 wt.%, predissolved in *n*-methyl-pyrrolidone) on an aluminum foil (30 um thick) current collector. The electrode was first dried at 60°C overnight in a blast oven, then tranferred to a vacuum oven and dried at 120 °C for 10 h (0.1 MPa). The electrolyte was 1 M $LiPF_6$ dissolved in a mixture of ethylene carbonate/diethyl carbonate/ethyl-methyl carbonate (EC/DEC/DMC = 1:1:1, by volume ratio). The charge-discharge behavours were measured by using a NEWARE BTS-6 10 test system (Shenzhen, China, 1C = 250 mA g^{-1}) at 25°C in the range of 2.0 and 4.8 V (vs. Li^+/Li). Electrochemical impedance spectra (EIS) of the as-assembled half cells were measured by using an CHI660a electrochemical station. The amplitude of AC was 5 mV and the frequency was set in the range from 100 kHz to 10 mHz.

3. RESULTS AND DISCUSSION

The XRD patterns of precursor, LMNO and PPy-LMNO are shown in Figure 1. The main peaks of the precursor indicate a mixture of metal carbonates [21]. All the strong diffraction peaks of

LMNO can be well indexed to a hexagonal α-$NaFeO_2$ structure (*R*-3*m* space group), while weak peaks between 20° and 23° could be ascribed to the super lattice structure of Li_2MnO_3 component (*C*2/*m* space group) [22,23]. Meanwhile, the adjacent peaks of (006)/(102) and (108)/(110) exhibits obvious splitting, confirming a highly ordered layered structure [24]. The peaks of PPy-LMNO have no obvious differences with the ones of LMNO, indicating no impure phase was emerged during coating process. The characterized peaks of PPy cannot be observed.

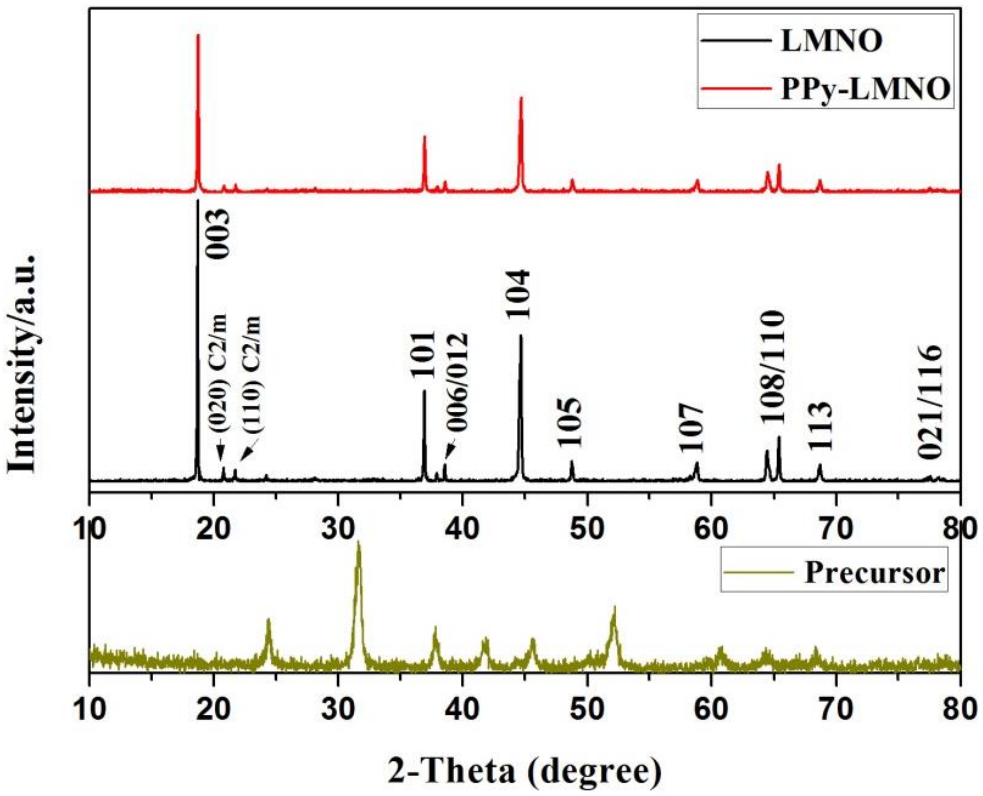

Figure 1. XRD patterns of precursor, LMNO and PPy-LMNO.

TG analysis was carried out in the air from 25°C to 800 °C with a heating rate of 5 °C min^{-1} to ascertain the quantity of PPy in PPy-LMNO, as shown in Figure 2a. It is reported that pure PPy burns out at 550 °C [17]. A mass loss process below 550 °C can be observed in Figure 2a, which is consistent with the burning of PPy. According to the curve, the mass fraction of PPy in PPy-LMNO is 2.5%. It is so small mass ratio that the characterized peaks of PPy cannot be seen in XRD pattern.

Raman tests were performed to confirm the formation of PPy in the PPy-LMNO. Figure 2b shows Raman spectroscopy of LMNO and PPy-LMNO. The peaks between 300 and 800 cm^{-1} are similar for two patterns. The two broad peaks around 607 cm^{-1} and 490 cm^{-1} are ascribed to Raman-active layered lithium transition metal oxide with *R*-3*m* space group. Another small Raman peak between 415 and 430 cm^{-1} originated from the fingerprint vibration of Li_2MnO_3 short-range

superlattice ordering [25,26]. A weak peak can be seen around 560 cm^{-1}, which indicated the existence of spinel phase [27]. However, there is no clear diffraction peaks of spinel phase in the XRD patterns shown in Figure 1, indicating only a trace of spinel nanodomains can be found in the sample. The Raman bands at around 1592 cm^{-1} ascribes to the vibrational band characteristic of oxidized state for PPy, which is associated with a mixed *v*C=C and interring *v*C-C vibration of short conjugation lengths. In addition, the peaks at around 1330, 1258 and 1060 cm^{-1} are related to the ring deformation mode and the peaks about 931 cm^{-1} are correlated to C-H out-of-the-plane deformation [19,28].

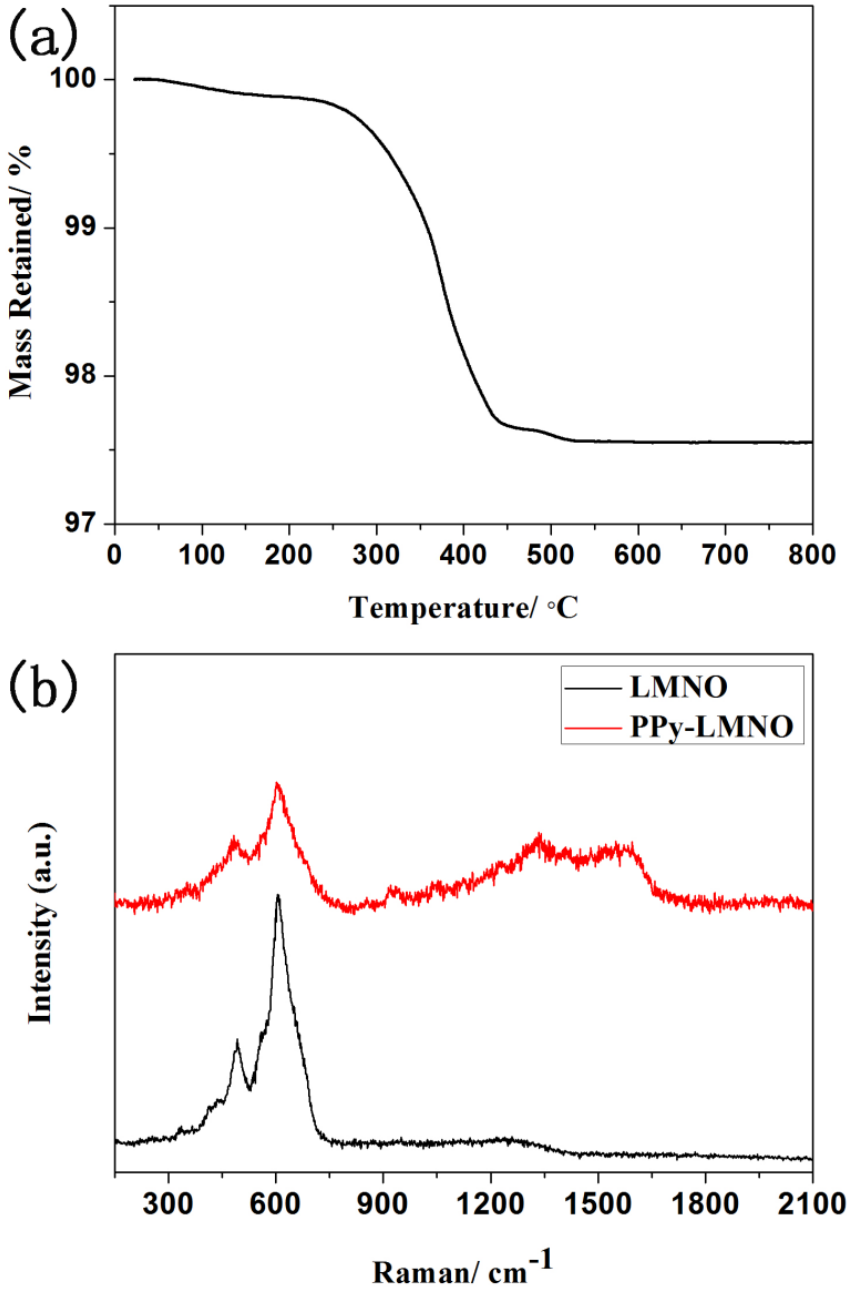

Figure 2. (a) TG curve of PPy-LMNO in air atmosphere with a heating rate of 5 °C min^{-1} and (b) Raman spectra of LMNO and PPy-LMNO.

Figure 3a-c shows the SEM images of the precursor, LMNO and PPy-LMNO. The precursor displays spherical shape with the diameter of about 200-500 nm. After high-temperature heating treatment, the spheres crack and form uniform nanoparticles around 100-200 nm. PPy-LMNO exhibits similar morphologies compared with LMNO, except for slightly rough surface caused by PPy coating on the surface of LMNO nanoparticles. High-resolution TEM images of PPy-LMNO are shown in Figure 3d. It can be obviously observed a thin amorphous layer on the surface with 3-5 nm. The lattice fringe distance of 0.47 nm is well indexed to the interplanar distance for both (003) of hexagonal phase (*R*-3*m*) and the (001) of monoclinic phase (*C*2/*m*) [4].

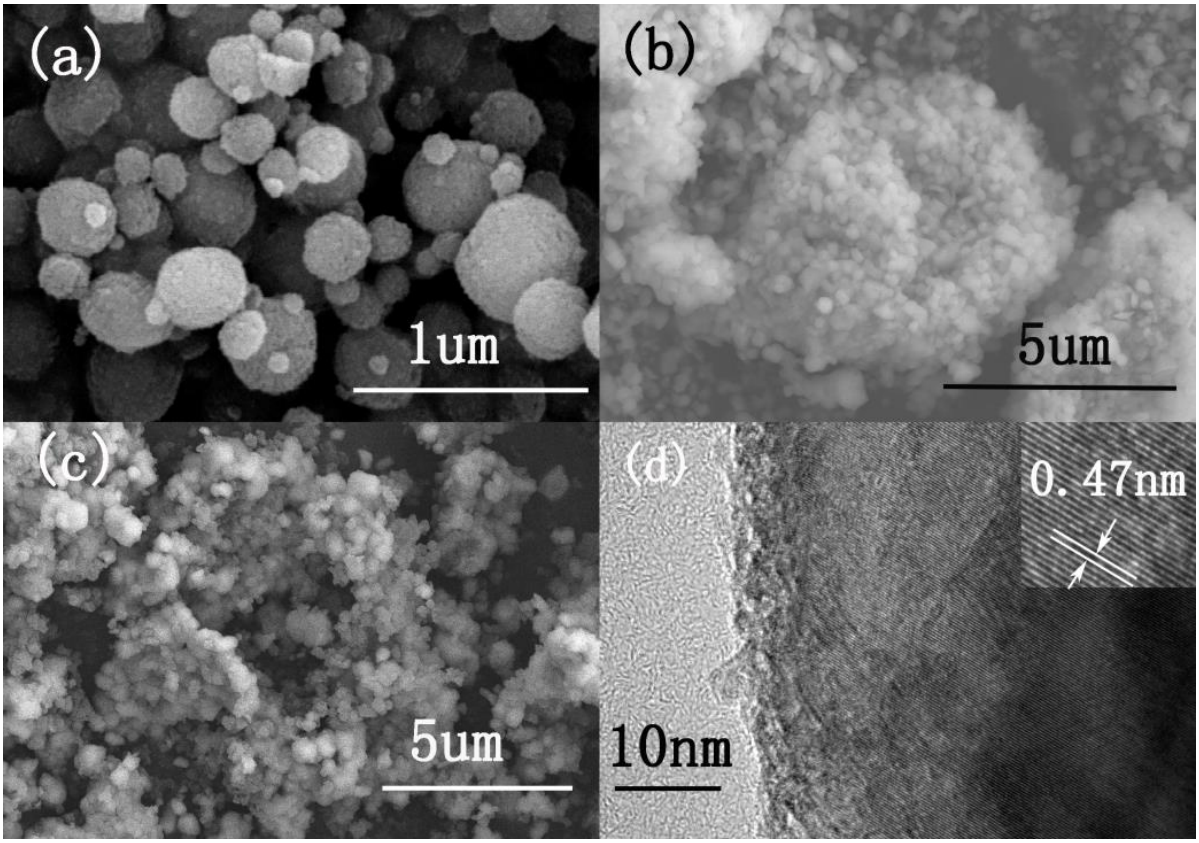

Figure 3. SEM images of the precursor (a), LMNO (b) and PPy-LMNO (c); (d) High-resolution TEM images of PPy-LMNO.

Figure 4 shows the charge-discharge profiles of the first two cycles for the LMNO and PPy-LMNO. Both initial charge curves consist of a slope below 4.5 V and a plateau region above 4.5 V, which indicate different Li-extraction mechanisms [29]. The low-voltage slope at 3.7-4.5 V is associated with the Li-extraction from the transition metal layered structure (R-3*m* space group), corresponding to the oxidation of Ni^{2+} to Ni^{4+} [5]. The plateau above 4.5 V is generally considered as simultaneous oxygen release with Li-extraction from the layered Li_2MnO_3 lattice corresponding to the

process of activation of Li_2MnO_3, which disappeared in the subsequent charge cycles and caused high initial irreversible capacity loss [30,31]. The initial charge and discharge capacities of LMNO and PPy-LMNO are 306.0/240.5 mAh g^{-1} and 285.3/236.8 mAh g^{-1} with the coulombic efficiencies of 78.6% and 83.0%, respectively. The initial charge capacity of PPy-LMNO is lower than that of LMNO, however, the initial coulombic efficiency is larger. It is probably ascribed that the PPy layer effectively reduces the contact between active material and electrolyte. However, the polarization is a little more obvious than bare LMNO, due to PPy coating layer does not facilitate the Li^+ ion transport at the surface of material.

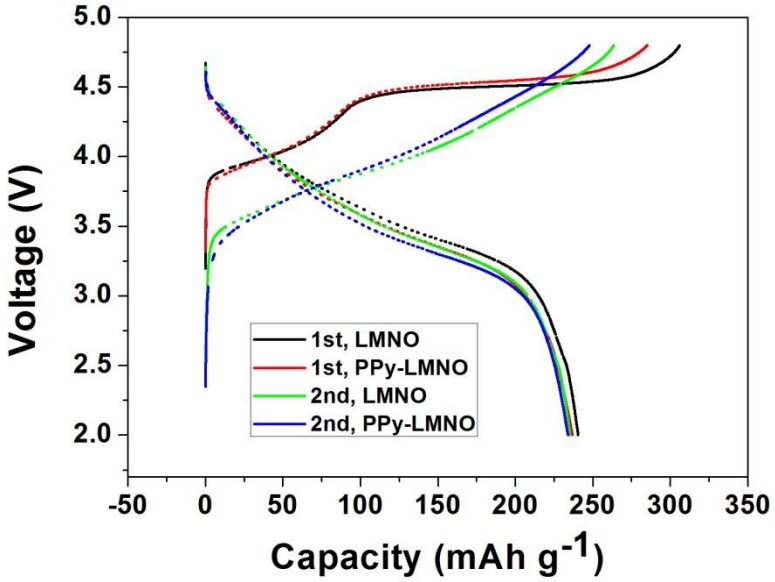

Figure 4. Charge-discharge profiles of initial two cycles for LMNO and PPy-LMNO at 0.1 C.

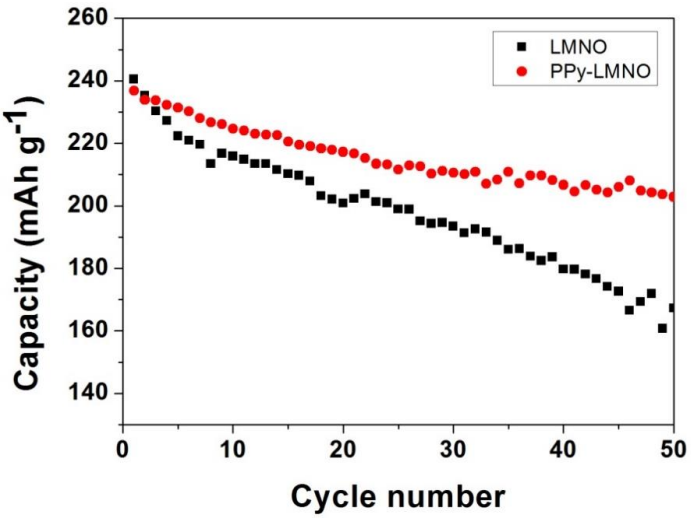

Figure 5. Cycle performance of LMNO and PPy-LMNO at 0.1 C in the voltage range of 2.0-4.8 V.

Table 1. Performances comparison of PPy-LMNO with some other Li-rich cathode materials

	Initial capacity (mAh g^{-1})	Retention	Ref.
PPy-LMNO	236.8 at 25 mA g^{-1}	85.7% after 50 cycles	This work
$Li_{1.2}Mn_{0.4}Co_{0.4}O_2$ by gel-combustion synthesis	208.6 at 20 mA g^{-1}	51.0% after 30 cycles	[32]
$Li_{1.2}Mn_{0.6}Ni_{0.2}O_2$ by solvothermal method	256.4 at 25 mA g^{-1}	47.8% after 100 cycles	[2]
MgO coated $Li_{1.2}Mn_{0.54}Ni_{0.13}Co_{0.13}O_2$	207.3 at 200 mA g^{-1}	84.9% after 100 cycles	[33]
Sm_2O_3 modified $Li_{1.2}Mn_{0.56}Ni_{0.16}Co_{0.08}O_2$	234.5 at 200 mA g^{-1}	91.5% after 80 cycles	[34]
$Li_{1.2}Mn_{0.54}Ni_{0.13}Co_{0.13}O_2$ by sol-gel method	202.1 at at 25 mA g^{-1}	94.5% after 15 cycles	[35]

Figure 5 depicts cycle performance of $Li_{1.2}Mn_{0.6}Ni_{0.2}O_2$ before and after surface modification at 0.1 C. Samples LMNO and PPy-LMNO deliver the discharge capacities of 240.5 and 236.8 mAh g^{-1} in the first cycle and maintain 167.2 and 202.9 mAh g^{-1} in 50th cycle, with capacity retentions of 69.5 and 85.7% respectively. Performances comparison of PPy-LMNO with some other Li-rich cathode materials is presented in Table 1.Despite low discharge capacity, PPy-LMNO exhibits the best cycle stability than pristine LMNO. It is probably attributed that the contact between electrolyte and material is inhibited and the oxygen release is suppressed thereby the structure change is alleviated after surface modification by PPy.

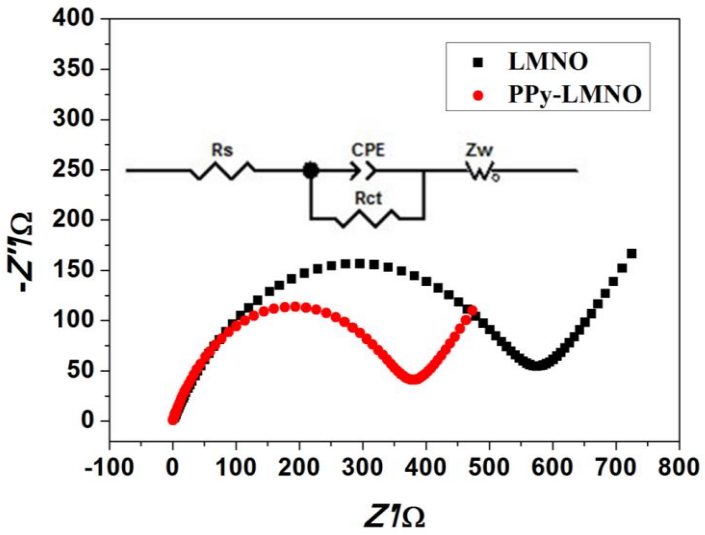

Figure 6. EIS spectra of LMNO and PPy-LMNO at 4.8 V after initial charging process.

EIS measurements of LMNO and PPy-LMNO were measured at 4.8 V after initial charging process. Figure 6 shows the Nyquist plots and equivalent electrical circuit of LMNO and PPy-LMNO electrodes. Here, R_s represents the resistance of the transportation of Li^+ through the interfacial film, R_{ct} is the charge transfer resistance. CPE means the constant phase element relating to double layer, Z_w describes the Warburg impedance which is related with diffusion of lithium ion in the particles. In Figure 6, A semicircle at high frequency and a slope line at low frequency are shown in Nyquist plots. Charge transfer resistance (R_{ct}) value of LMNO and PPy-LMNO are measured as 563.2 Ω and 375.8 Ω respectively, which shows PPy-LMNO exhibits a smaller charge transfer resistance. The charge transfer resistance is decreased after coating due to electronic conductivity of PPy.

4. CONCLUSIONS

In this work, Li-rich cathode material $Li_{1.2}Mn_{0.6}Ni_{0.2}O_2$ was prepared by solvothermal method and coated with 2.5 wt.% conducting polypyrrole. Surface modification improves the initial coulombic efficiency, the cyclic stability and electronic conductivity with a smaller charge transfer resistance, contributing to a better electrochemical performance. The corrosion of material surface from electrolyte at high potentials is restrained, the oxygen release is suppressed and the structure change is alleviated by PPy coating layer. It slightly sacrificed the initial capacity but highly improved the stability of $Li_{1.2}Mn_{0.6}Ni_{0.2}O_2$ cathode materials.

ACKNOWLEDGEMENTS

This work was supported by National Natural Science Foundation of China (51575030 and 51774017), Beijing Natural Science Foundation (2174075), Key Program of Equipment Pre-Research Foundation of China (6140721020103) and Scientific Research Foundation of SGCC (52170217000L).

References

1. W. Yan, H. Wen, Y. Chen, Y. Wang and Y. Liu, *Journal of Power Sources,* 277 (2015) 76.
2. Q. Zhang, T. Peng, D. Zhan and X. Hu, *Journal of Power Sources,* 250 (2014) 40.
3. S.-H. Yu, T. Yoon, J. Mun, S. Park, Y.-S. Kang, J.-H. Park, S. M. Oh and Y.-E. Sung, *J. Mater. Chem. A,* 1 (2013) 2833.
4. M. M. Thackeray, S.-H. Kang, C. S. Johnson, J. T. Vaughey, R. Benedek and S. A. Hackney, *J. Mater. Chem.,* 17 (2007) 3112.
5. C. S. Johnson, J.-S. Kim, C. Lefief, N. Li, J. T. Vaughey and M. M. Thackeray, *Electrochemistry Communications,* 6 (2004) 1085.
6. Y. Lee, M. G. Kim and J. Cho, *Nano Lett.,* 8 (2008) 957.
7. X. Huang, Q. Zhang, H. Chang, J. Gan, H. Yue and Y. Yang, *Journal of Power Sources,* 156 (2009) A162.
8. X. Zhang, C. Yu, X. Huang, J. Zheng, X. Guan, D. Luo and L. Li, *Electrochimica Acta,* 81 (2012) 233.

9. A. Abouimrane, O. C. Compton, H. Deng, I. Belharouak, D. A. Dikin, S. T. Nguyen and K. Amine, *Electrochem. Solid-State Lett.*, 14 (2011) A126.
10. X. Jin, Q. Xu, H. Liu, X. Yuan and Y. Xia, *Electrochimica Acta*, 136 (2014) 19.
11. X. Wei, S. Zhang, Z. Du, P. Yang, J. Wang and Y. Ren, *Electrochimica Acta*, 107 (2013) 549.
12. Y. J. Hong, J. H. Kim, M. H. Kim and Y. C. Kang, *Materials Research Bulletin*, 47 (2012) 2022.
13. F. Fu, Y. Huang, P. Wu, Y. Bu, Y. Wang and J. Yao, *Journal of Alloys and Compounds*, 618 (2015) 673.
14. X. Xiang, X. Li and W. Li, *Journal of Power Sources*, 230 (2013) 89.
15. F. Fu, Q. Wang, Y.-P. Deng, C.-H. Shen, X.-X. Peng, L. Huang and S.-G. Sun, *J. Mater. Chem. A*, 3 (2015) 5197.
16. C. Wu, X. Fang, X. Guo, Y. Mao, J. Ma, C. Zhao, Z. Wang and L. Chen, *Journal of Power Sources*, 231 (2013) 44.
17. J. Cao, G. Hu, Z. Peng, K. Du and Y. Cao, *Journal of Power Sources*, 281 (2015) 49.
18. P. Zhang, L. Zhang, X. Ren, Q. Yuan, J. Liu and Q. Zhang, *Synthetic Metals*, 161 (2011) 1092.
19. X.-W. Gao, Y.-F. Deng, D. Wexler, G.-H. Chen, S.-L. Chou, H.-K. Liu, Z.-C. Shi and J.-Z. Wang, *J. Mater. Chem. A*, 3 (2015) 404.
20. X. Xiong, D. Ding, Z. Wang, B. Huang, H. Guo and X. Li, *J Solid State Electrochem*, 18 (2014) 2619.
21. D. Luo, G. Li, C. Fu, J. Zheng, J. Fan, Q. Li and L. Li, *Adv. Energy Mater.*, 4 (2014) 1400062.
22. M. M. Thackeray, C. S. Johnson, J. T. Vaughey, H. N. LiCurrent address: eVionyx Inc. and S. A. Hackney, *J. Mater. Chem.*, 15 (2005) 2257.
23. A. D. Robertson and P. G. Bruce, *Chem. Mater.*, 15 (2003) 1984.
24. J. Lin, D. Mu, Y. Jin, B. Wu, Y. Ma and F. Wu, *Journal of Power Sources*, 230 (2013) 76.
25. J. Liu, J. Yang, S. Guo, Y. Wang, C. Wang, H. Liu, Q. Xu and Y. Xia, *Surf Technol*, 44 (2015) 15.
26. E. Proietti, F. Jaouen, M. Lefèvre, N. Larouche, J. Tian, J. Herranz and J.-P. Dodelet, *Nature communications*, 2 (2011) 416.
27. J. Hong, D.-H. Seo, S.-W. Kim, H. Gwon, S.-T. Oh and K. Kang, *J. Mater. Chem.*, 20 (2010) 10179.
28. M.J.L. Santos, A. G. Brolo and E. M. Girotto, *Electrochimica Acta*, 52 (2007) 6141.
29. J.-S. Kim, C. S. Johnson, J. T. Vaughey, M. M. Thackeray, S. A. Hackney, W. Yoon and C. P. Grey, *Chem. Mater.*, 16 (2004) 1996.
30. Z. Lu and J. R. Dahn, *Journal of Alloys and Compounds*, 149 (2002) A815.
31. S. J. Shi, J. P. Tu, Y. Y. Tang, Y. Q. Zhang, X. L. Wang and C. D. Gu, *Journal of Power Sources*, 240 (2013) 140.
32. C. Fu, G. Li, D. Luo, J. Zheng and L. Li, *J. Mater. Chem. A*, 2 (2014) 1471.
33. S. J. Shi, J. P. Tu, Y. Y. Tang, X. Y. Liu, Y. Q. Zhang, X. L. Wang and C. D. Gu, *Electrochimica Acta*, 88 (2013) 671.
34. S. J. Shi, J. P. Tu, Y. J. Zhang, Y. D. Zhang, X. Y. Zhao, X. L. Wang and C. D. Gu, *Electrochimica Acta*, 108 (2013) 441.
35. P. Yang, S. Zhang, X. Wei, J. Meng, and Y. Xing, *Int. J. Electrochem. Sci.*, 10 (2015) 9424.